5-1-2007

Electrochemical Detection of Prostate Carcinoma Biomakers Using Nanotechnology

Kathryn Leonard
Salve Regina University

Chapter 1

Introduction

1.1 Purpose of Study

Even with advances in cancer research and technology cancer is the second leading cause of death in the United States as no cure exists[1]. According to the latest America Cancer Society statistics[2], this year alone nearly 560,000 people will die from the disease. Of the total 1.45 million that will be diagnosed, 218,000 will be prostate carcinoma and over 27,000 cases will result in death[2]. There is, however, a strong connection between early detection and positive patient outlook. In the case of lung cancer there is a 70% survival rate for resected infected tissue in stage I carcinoma versus only 12% when the cancer is not detected in this stage[3]. Besides lung carcinoma, early detection is the best hope in all cancers, to improve patient survival, disease prognosis and may lead to cancer prevention.

The major goal of this research is to develop a rapid, ultrasensitive, economic, and specific nanomaterial-based sensor for the early detection of cancer biomarker proteins, particularly Prostate Specific Antigen (PSA), in clinically relevant samples, such as serum and tissue lysate. In this research study, we are using vertically aligned single-walled carbon nanotubes (SWNT) attached to conductive surfaces capable of electrical conduction to fabricate these ultrasensitive sandwich immuosensors. The electrical signal

---

[1] Ahmedin Jemal, Taylor Murray, Elizabeth Ward, Alicia Samuels, Ram C. Tiwari, Asma Ghafoor, Eric J. Feuer, Michael J. Thun. *CA Cancer J. Clin*. **2005,** *55(1)*, 10-30.

[2] Estimated New Cancer Cases and Deaths by Sex for All Sites, US, 2007. American Cancer Society. 2007. 15 Apr. 2007 <http://www.cancer.org/downloads/stt/CFF2007EstCsDths07.pdf>.

[3] Henschke, Claudia; Dorthy I. McCauley, David F. Yankelevitz, David P Naidich, Gergeann McGuiness, Olli S. Miettinen, Daniel M. Libby, Mark W. Pasmantier, June Koizumi, naser K. Altorki, James P. Smith. *The Lance.* **1999**, *354,* 99-105.

is realized using enzyme catalytic reactions involving Horseradish Peroxidase (HRP) tracer in the antibody-antigen biorecognition event.

This project employs SWNT with ~1.4 nm diameters and the world's highest conductivity per unit mass[4]. We have combined efficient electrical transduction by shortened carbon nanotubes with biomolecular recognition by antibodies. Electronic devices offer elegant ways for interfacing biorecognition and transduction events and are uniquely qualified for meeting the high sensitivity and portability requirements of future biodetection systems[5,6]. Electrochemical bioassays involving enzyme tracers have received particular attention due to the intrinsic signal amplification provided by biocatalytic reactions.

An important future goal of this project is to develop a protein sensor array that is capable of measuring a collection of cancer biomarker proteins in a single sample. This array would allow for lower cost per analysis and a clinically viable approach for early cancer detection. The onset of cancer is indicated by biomarker serum level change over time[7]. These biomarkers often indicate at abnormal levels, or abnormal level changes over time, a disturbance in the proper regulation of a specific tissue or organ often indicating carcinoma[8].

---

[4] Dresselhaus, M. S.; Dresselhaus, G.; Avouris, P.; Editors, Carbon nanotubes: Synthesis, Structure, Properties, and Applications. *Topics Appl. Phys*., **2001**.
[5] Palecek, E.; Fojta, M. Detecting DNA hybridization and damage. *Anal. Chem.* **2001**, *73*, 75A.
[6] Wang, J. Real-time electrochemical monitoring: toward green analytical chemistry. *Acc. ChemRes.***2002**, *35*, 811.
[7] Brosman, Stanley A. "Prostate Specific Antigen." EMedicine From WebMD. 15 June 2006. University of California Los Angeles Medical School. 23 Mar. 2007
[8] Weston, A.D.; Hood, L. *J. Proteome Res*. **2004**, *3*, 179-196.

Currently there are many methods for detection of proteins, however all have many drawbacks. DNA microarrays measure gene expression by quantifying messenger RNA levels. However, these mRNA levels are not indicative of protein expression[8]. Protein microarrays, specifically ELISA, are another similar method where antibodies and enzyme-labeled secondary antibodies are used in a sandwich immunoassay. This method is selective and sensitive but is limited by the required sample size and time[9].

Mass spectrometry (MS) is yet another method for protein detection. This technique requires liquid chromatograph protein purification, proteolytic cleavage of peptide chains and labeling with isotopes for analysis, which is labor-intensive and expensive[10]. This is an unlikely method for mass sampling in a timely and reasonably priced manner.

This innovative immunosensor design would lead to a miniaturized electrochemical immunosensor arrays with higher throughput and lower cost per analysis. Such a device would be a clinically viable approach for early cancer detection compared to expensive and complex MS methods. We believe that the SWNT protein microarrays offer unprecedented promise for early cancer diagnosis.

Chapter 2 of this thesis describes peroxidase activity of horseradish peroxidase and myoglobin on vertically aligned carbon nanotubes; key steps in the electrochemical detection scheme. These initial studies were intended to establish the optimum conditions for the SWNT "forest" fabrication and also serve as quality control experiments to

[9] Wilson, D.S.; Nock, S. *Angew. Chem. Int. Ed.* **2003**, *42*, 494-500
[10] Aebersold, Ruedi; Goodlet, David. *Chem. Review.* **2001**, *101*, 269-295

determine the quality of our SWNT forests. Electrode-driven peroxidase activity of myoglobin and horseradish peroxidase attached to the carbon nanotube arrays was demonstrated, with detection limits for hydrogen peroxide in buffer solutions of ~100 nM. Our results suggest that the vertically aligned nanotube arrays behave like metal electrical conductors shuttling electrons from the external circuit to redox active sites of the enzymes.

Chapter 3 demonstrates our novel nanomaterial-based sensor for use in electrochemical detection of prostate specific antigen. We obtained a detection limit of 0.4 ng/mL, which compares favorably with common methods such as enzyme-linked immunosorbent assay (ELISA). Work is currently in progress to lower the detection limits using signal amplification strategies, the established optimized SWNT array fabrication protocol and conditions for minimal non-specific binding events.

Finally, chapter 4 addresses the Pell honors program connection with this research work. As a Pell student, with the goal of learning to understand the importance of international relations and public policy, I have found through this research experience that early detection of cancer biomarkers is a key step towards improving cancer patient's survival and may even lead to cancer prevention. Increasing the sensitivity of the detection methods would indicate this early detection and therefore would be essential in lowering healthcare costs for cancer patients as treatments would be much less invasive and time consuming. Detection of high levels of PSA in serum can lead to detection of prostate cancer well before surgery is required, resulting in much less aggressive, more successful treatments that minimize patient discomfort and physiological dysfunction.

1.2 Prostate Specific Antigen

PSA is a single chain glycoprotein from the Kallikrein family of proteolyses[11]. It is composed of a 237 amino acid chain having a molecular weight of 26kDa[12]. PSA has multiple epitopes capable of binding with monoclonal antibodies, which in this research is essential to its detection[13]. PSA is a known biomarker for the detection of prostate cancer[8]. The detection of PSA rising levels allows for a probable diagnosis of prostate cancer.

1.3 Carbon nanotubes

Single-Wall carbon nanotubes (SWNTs) are essentially a seamless cylinder of graphene. The tubes are capable of acting as conductors or semiconductors depending on the chiral alignment of the molecules. These one-dimensional fibers exhibit electrical conductivity as high as copper, thermal conductivity as high as diamond, strength 100 times greater than steel at one sixth the weight, and high strain to failure (high aspect ratio)[14]. There are two types of carbon nanotubes, SWNT and multi-wall carbon nanotubes (MWNT). MWNT possess the properties of the SWNTs but are composed of one graphene cylinder inside of another.

The SWNTs used in this experiment are capable of single electron conduction. At 1.4nm diameter SWNTs have the highest conductivity per unit mass in the world. The SWNT

[11] RCSB Protein Data Bank. wwwPDB. 15 Apr. 2007 <http://www.rcsb.org/pdb/explore.do?structureId=1GVZ>.
[12] Belanger, A; H Van Halbeek; HC Graves; K Grandbois; Ta Stamey; L Huang; I Poppe; and F Labrie. *Prostate* **1995**, *27*, 187-197
[13] Leinonen, J.; Wu, P.; Stenman, U. *Clinical Chemistry*. **2002**, *48*, 2208-2216.
[14] "Nanotubes and Buckyballs." Nanotechnology Now. 15 Aug. 2006. 7 Mar. 2007 <http://www.nanotech-now.com/nanotube-buckyball-sites.htm>.

used in this work are carboxyl functionalized by acid treatment and are capable of attachment of biological molecules by bioconjugation reactions. Due to their unique structural, electronic, thermal, and mechanical properties they have found wide

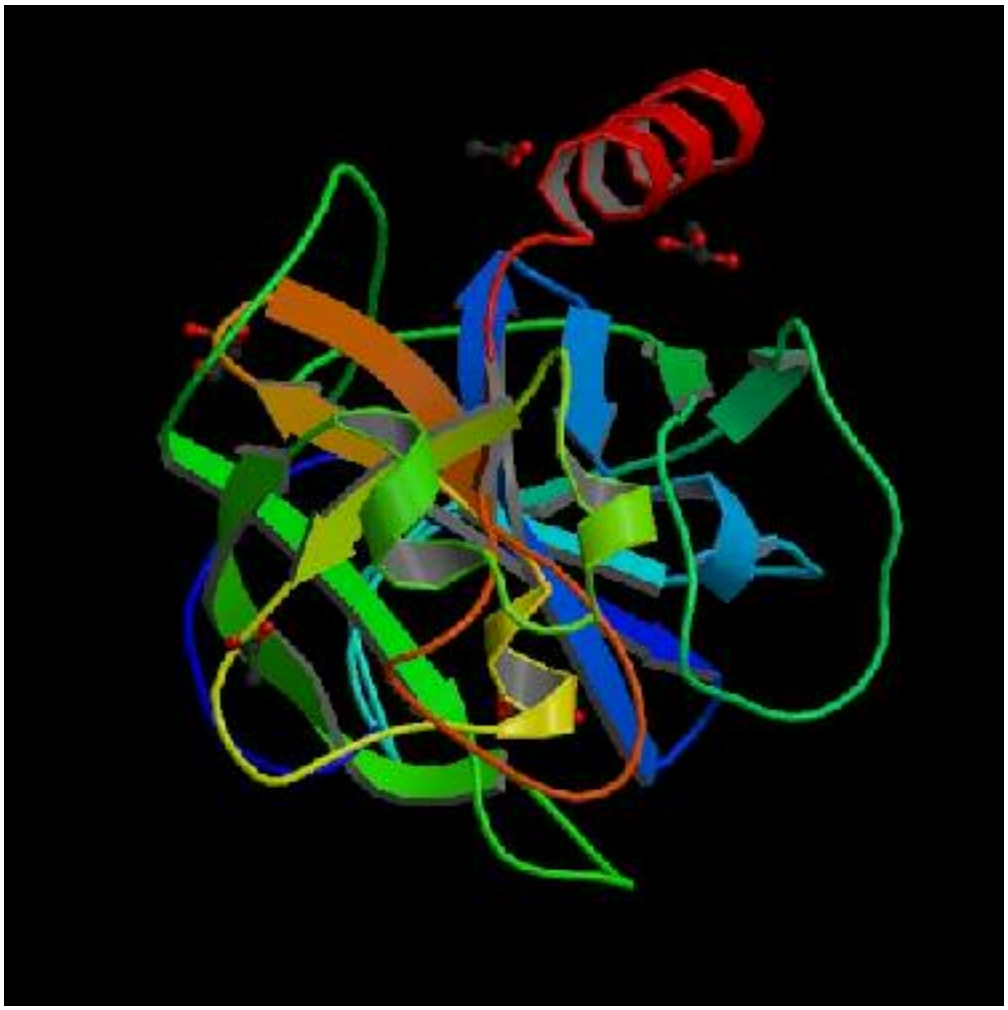

Figure 1-1.Prostate Specific Antigen structure as determined by x-ray diffraction[15].

[15] RCSB Protein Data Bank. wwwPDB. 15 Apr. 2007 <http://www.rcsb.org/pdb/explore.do?structureId=1GVZ>.

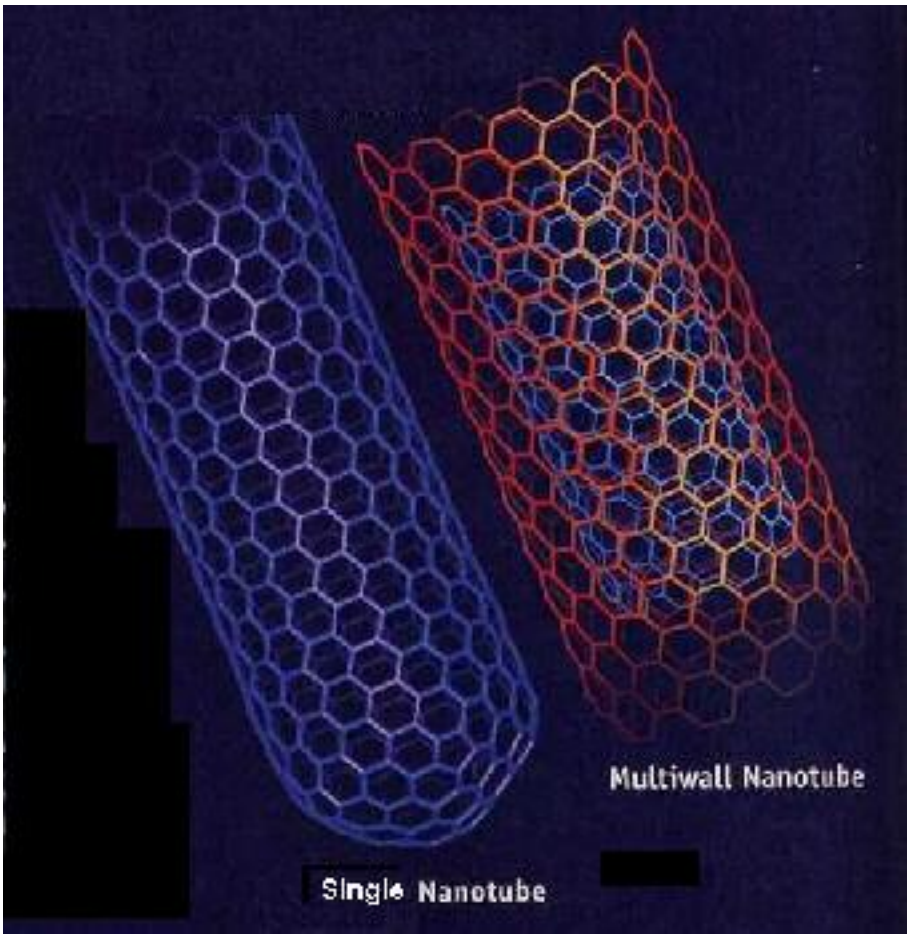

Figure 1-2. Two type of carbon nanotubes, SWNT and MWNT

applications in various bioanalytical applications including electrochemical detection by cyclic voltammetry and amperometry.

1.4 Horseradish Peroxidase

Horseradish peroxidase (HRP) is a member of the ferroprotoporphyrin group of peroxidases. It is a single chain polypeptide containing a central heme group. This heme group is capable of catalytic oxidation reduction by hydrogen peroxide[16]. Peroxidases have been used extensively for sensitive electrochemical detection in immunosensing[17,18,19] and DNA hybridization[5,20,21]. They are excellent labels for electrochemical immunoassays since highly active peroxidases give large catalytic electrochemical signals for reduction of hydrogen peroxide at low applied voltages where little interferences is expected[22,23].

---

[16] "Peroxidase Enzymes and Reagents." Enzyme Explorer. 2007. Sigma-Aldrich. 15 Apr. 2007 <http://www.sigmaaldrich.com/Area_of_Interest/Biochemicals/Enzyme_Explorer/Analytical_Enzymes/Peroxidase_Enzymes.html>.

[17] Lu, B.; Iwuoha, E. I.; Smyth, M. R.; O'Kennedy, R. Development of an amperometric immunosensor for horseradish peroxidase (HRP) involving an non-diffusional osmium redox polymer co-immobilized with anti-HRP antibody, *Anal. Commun*. **1997**, 34, 21-23.

[18] Killard, A. J.; Zhang, S.; Zhao, H.; John, R.; Iwuoha, E. I.; Smyth, M. R. *Anal. Chim. Acta* **1999**, *400*, 109-119.

[19] Killard, A. J.; Micheli, L.; Grennan, K.; Franek, M.; Kolar, V.; Moscone, D.; Palchetti, I.; Smyth, M. R. *Anal. Chim. Acta* **2001**, *427*, 173-180.

[20] Azek, F.; Grossiord, C.; Joannes, M.; Limoges, B.; Brossier, P. *Anal. Biochem.* **2000**, *284*, 107-113.

[21] Caruana, D. J.; Heller, A. *J. Am. Chem. Soc*. **1999**, *121*, 769-774.

[22] Ruzgas, T.; Lindgren, A.; Gorton, L.; Hecht, H.-J.; Reichelt, J.; Bilitewski, U. in Chambers, J. Q. and Bratjer-Toth, A. Eds. *Electroanalytical Methods for Biological Materials,* Marcel Dekker, New York, **2002**, pp. 233-254.

[23] Guo, Y.; Guadalupe, A. R. Direct electrochemistry of horseradish peroxidase adsorbed on glassy carbon electrode from organic solutions. *Chem. Comm*. **1997**, 1437-1438.

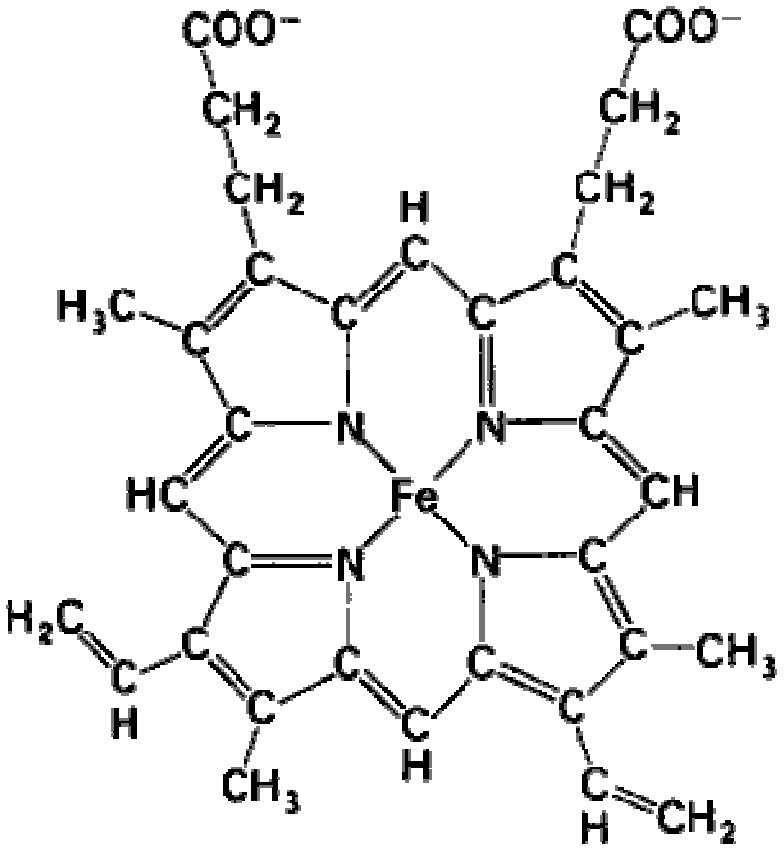

Heme
(Fe-protoporphyrin IX)

Figure 1-3. Heme group of Horseradish Peroxidase[24].

[24] Prahl, Scott. "Structure of Heme." 8 June 1998. Oregon Medical Laser Center. 20 April 2007. <http://omlc.ogi.edu/spectra/hemoglobin/hemestruct/index.html>.

Chapter 2

Peroxidase Activity of Horseradish Peroxidase and Myoglobin on Vertically Aligned Carbon Nanotubes

2.1. Abstract

2.2. Introduction

Arrays of highly conducting single-wall carbon nanotubes (SWNTs) could be uniquely suited for bioanalytical applications by coupling sensing biomolecules to the carboxyl-terminated ends[25,26] of the nanotubes. There are a number of established methods for assembling 20-100nm vertically aligned carbon nanotube arrays on surfaces in nm-scale bundles called SWNT forests i.e., dense orthogonally oriented arrays of shortened SWNTs, onto various solid substrates [27, 28, 29]. In agreement with our first major goal in this research work to optimize the SWNT forest assembly, and biomolecular bioconjugation, we herein demonstrate successful fabrication of vertically aligned SWNT arrays. Furthermore, we show that the untethered ends of these stable SWNT forests can be linked to electrochemically active heme proteins through traditional bioconjugate chemistry to give electrochemical signatures of enzyme activity. In this work, we clearly show that myoglobin and horseradish peroxidase covalently linked to the SWNT forests exhibit quasi-reversible Fe^{III}/Fe^{II} voltammetry and sensitive responses to H_2O_2. The unidimensional nature, high conductivity, and structural robustness of carbon nanotubes

[25] Liu, Jie; Andrew G. Rinzler, Hongjie Dai, Jason H. Hafner, R. Kelley Bradley, Peter J. Boul, Adrian Lu, Terry Iverson, Konstantin Shelimov, Chad B. Huffman, Fernando Rodriguez-Macias, Young-Seok Shon, T. Randall Lee, Daniel T. Colbert, and Richard E. Smalley *Science* **1998**, *280*, 1253

[26] Hamon, M.A.; H. Hu, P. Bhowmik, S. Niyogi, B. Zhao, M. E. Itkis, R. C. Haddon Chem. Phys. Lett. **2001**, *347*, 8.

[27] D. Chattopadhyay, I. Galeska and F. Papadimitrakopoulos; *J Am. Chem. Soc*. **2001**, *123*, 9451.

[28] Gooding, J; W. Rahmat, J. Q. Liu, W. R. Yang, D. Losic, S. Orbons, F. J. Mearns, J. G. Shapter, D. B. Hibbert. *J Am. Chem. Soc*. **2003**, *125*, 9006.

[29] Patolsky, F.; Y. Weizmann, I. Willner, *Chem. Int. Edition* **2004**, *43*, 2113

promise important future applications for nanosensors. Unique electrochemistry of soluble molecules and adsorbed proteins on cast flat non-oriented layers of single of multi-walled carbon nanotubes has been demonstrated[30,31]. It has been speculated that the similarity between size scales of enzymes and chemically shortened, nanoscale diameter SWNTs might promote the likelihood of SWNTs being able to intimately interact and be within electron tunneling distance of enzyme redox sites[32].

2.3. Experimental Section

Single-wall carbon nanotubes (HiPco, from Tubes@ rice) were carboxyl functionalized and shortened by sonication in a mixture of 3:1 HNO_3 and H_2SO_4 for 4 h at 70ºC[27]. Monolayers of vertically aligned, shortened SWNTs were assembled on ordinary pyrolytic graphite (PG) electrodes from DMF dispersions onto an underlying composite bed of Nafion ionomer and Fe^{3+}-precipitated hydroxides, as described previously[27]. SWNTs on the Nafion–$Fe(OH)_3$ layer on PG were dried in vacuo for 18 h. Cyclic voltammetry and amperometry were done as previously described.

Atomic force microscopy (AFM) was done with a Nanoscope IV scanning probe microscope. Iron heme proteins horse heart myoglobin (Mb, Sigma, >90%) and horseradish peroxidase (HRP, Sigma, 250–330 unit mg-1) were attached onto the ends of the SWNTs in the forest by using the water-soluble carbodiimide, (1-(3-(dimethylamino)propyl)-3-ethylcarbodiimide hydrochloride, EDC), to promote amide linkages between the carboxyl-terminated nanotubes and the lysine residue of the

[30] Campbell, J.K.; Sun, L.; Crooks, R.M. *J. Am. Chem. Soc.,* **1999**, *121*, 3779.
[31] Salvetat, J.P; AJ Kulik, JM Bonard, G Andrew, D Briggs, T Stockli. J. *Adv. Mater*. **1999**, *11*, 54.
[32] Baughman, R. *Nanotechnology* **2002**, *13*, 559.

proteins. This was done by placing a 20 μL droplet of freshly prepared 24 mM EDC in water onto the SWNT forest, immediately followed by adding 30 μL of 3 mg mL-1 Mb or HRP. EDC and protein solutions were mixed carefully using a syringe needle, reacted for 4 h, then washed extensively with water.

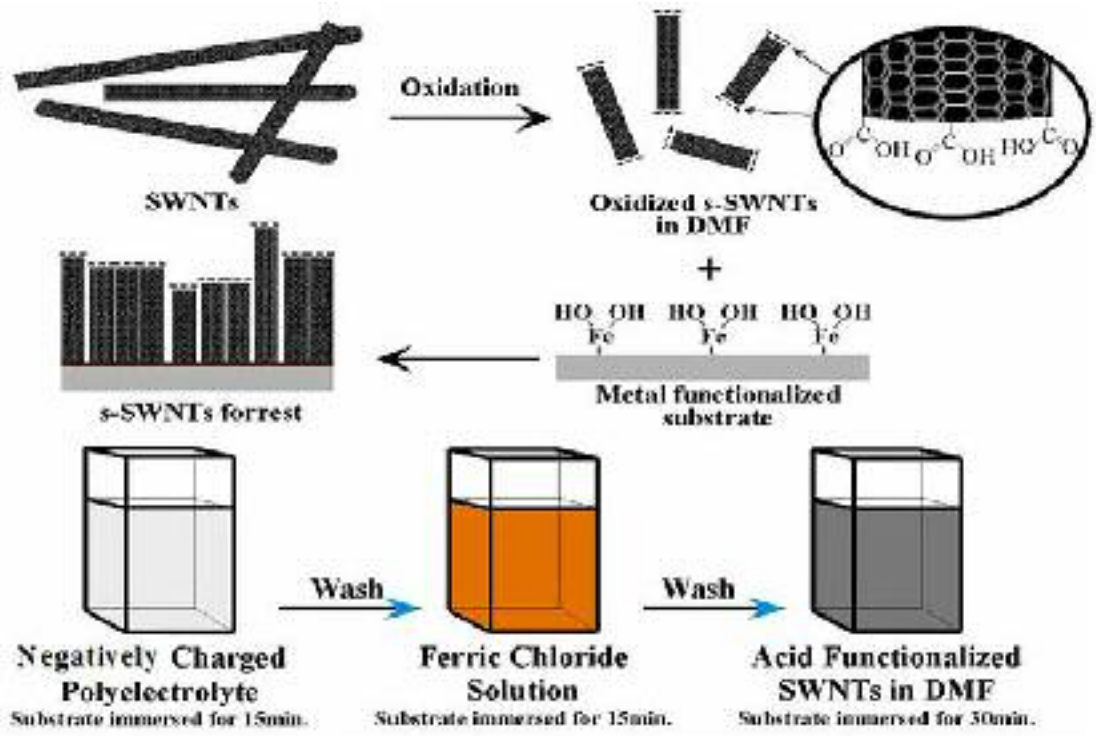

Figure 2-1. Schematics of the fabrication protocol of the vertically aligned SWNT arrays. End carboxyl group on the SWNT allow protein bioconjugation facilitating electron shuttle to active protein redox sites.

2.4. Results and Discussion

The SWNT forest construction was optimized using Resonance Raman spectroscopy and Atomic force Microscopy (AFM). The Raman spectra gave high intensity bands corresponding to graphite- (G-) and defects- (D-) bands respectively. The D-bands typically observed between 1250 and 1450 cm^{-1}, originate from the first order scattering by in-plane hetero-atom substituents, grain boundaries, vacancies or the other defects and by finite size defects[33]. Raman spectroscopy also shows peaks at 230 cm^{-1}, which is characteristic of radial breathing mode (RBM) of SWNT in the Nafion/$Fe(OH)_3$/SWNT assembly. This peak is absent in Nafion/$Fe(OH)_3$ confirming successful assembly of the SWNT arrays. The pH of the $FeCl_3$ solution was shown to play a key role in the successful fabrication of the SWNT forest. Raman spectroscopy shows clearly that the optimum pH =1.7 gave 100% SWNT coverage which may be attributed to the formation of $Fe(OH)_3$ nanocrystals that acts a precursor for the metal chelation reaction with the carboxylated ends of the SWNT.

Figure 2-2 shows AFM images of a SWNT forest on smooth silicon. The width of the main features on the SWNT forest surface is about 20 nm, significantly larger than the diameter of a single 1 nm diameter SWNT. This is due to the aggregation of SWNT in the assembly process and the tip-induced broadening artifact of the AFM[34]. The height of the SWNTs is ~40-60 nm, in agreement with that reported previously[35]. Cyclic voltammograms (CVs) of SWNT forests (Fig. 2(d)) showed an oxidation–reduction peak

[33] Dresselhaus, MS, and PC Eklund. *Adv. Phys*. **2000**, *49*, 705.
[34] D. Chattopadhyay; S. Lastella; S. Kim; F. Papadimitrakopoulos. *J. Am. Chem. Soc*. **2002**, *124*, 223.
[35] Diao, Peng; Liu, Zhongfan; Wu, Bin; Nan, Xiaolin; Zhang, Jin; Wei, Zhong. *Chem. Phys. Chem*. *02/03*, **2002**, 898.

pair centered at 0.2 V vs. SCE that has been assigned to carboxylate on non-oriented SWNT films[36].

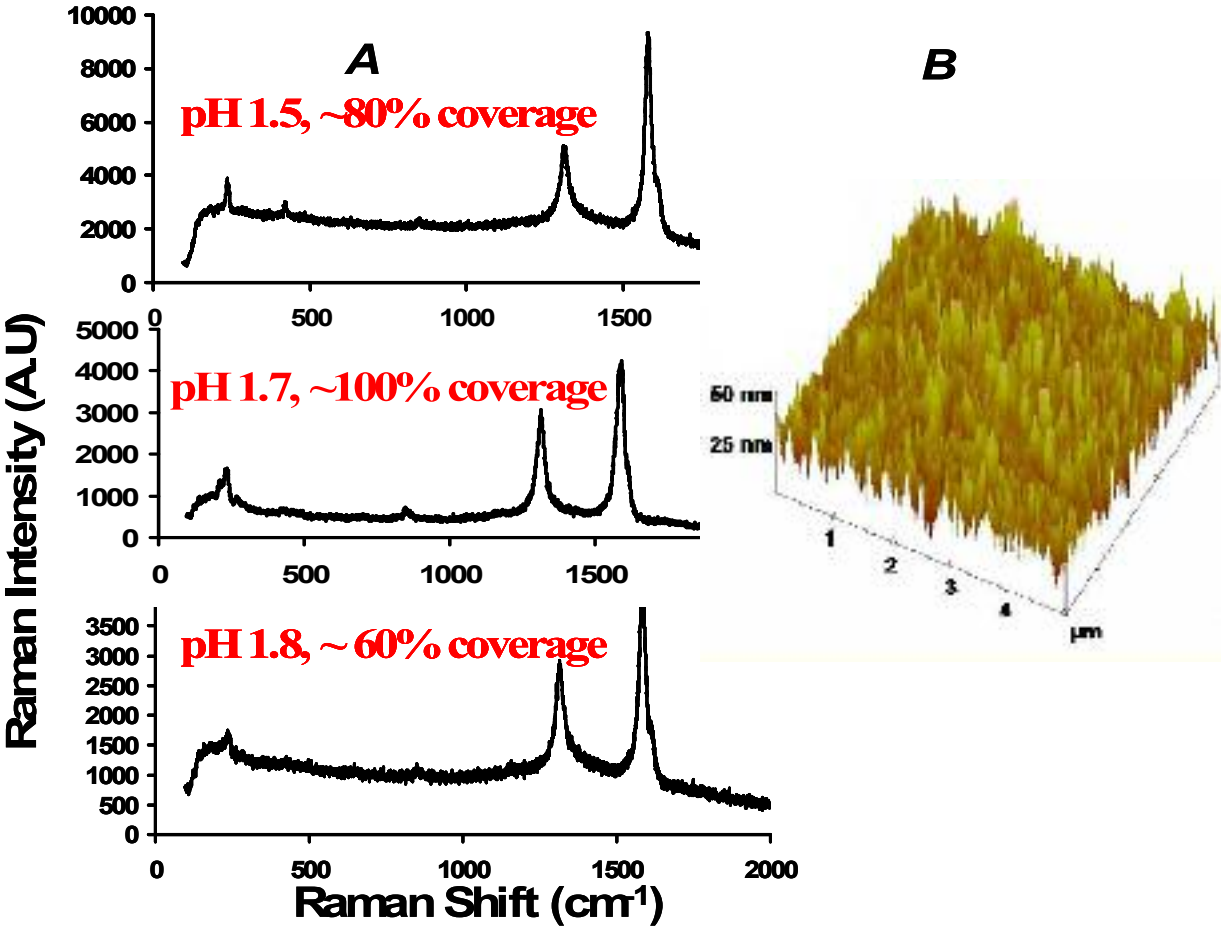

Figure 2-2. Raman spectra (A) showing characteristic D bands, G band and RBM band of SWNT assembled on PG electrodes and the influence of $Fe(Cl)_3$ solution pH during SWNT assembly, and (B) AFM image of the resulting vertically aligned SWNT arrays on Si wafers at the optimal pH 1.7.

[36] Luo, Hongxia; Shi, Zujin; Li, Nanqiang; Gu, Zhennan; Zhuang, Qiankun. *Anal. Chem*. **2001**, *73*, 915.

Addition of 0.1 mM H_2O_2 to the buffer resulted in an increase in the peak at -0.8 V, possibly due to the direct reduction of peroxide. Cyclic voltammograms of the protein–SWNT films in buffers showed oxidation–reduction peak pairs near -0.21 V vs. SCE for Mb, and -0.25 V for HRP. These potentials are characteristic of the Fe^{III}/Fe^{II} redox couples of Mb and HRP in thin films[37]. Furthermore, CV peaks of the SWNTs attributed to carboxylate disappeared from the CVs, suggesting that carboxyl groups on the SWNTs reacted during protein coupling. Separations between protein reduction and oxidation peaks were nearly zero. The peak current of the film increased linearly with increasing scan rate. All these results are typical of quasi-reversible voltammetry of a thin surface-confined layer of redox protein[38]. Electroactive protein surface concentrations were estimated by integrating the CV reduction peaks at low scan rates (25–75 mV s^{-1}). These surface concentrations were 0.17 nmol cm^{-2} for HRP and 0.09 nmol cm^{-2} for Mb, based on PG area (0.2 cm^2).

Cyclic voltammogram peaks of the enzymes attached onto SWNT forests were stable, and did not decay during repetitive multiple scans. Electrodes could be stored for several weeks in buffer at 4º C with only ~20% loss of peak current. This behavior is consistent with covalent attachment of the proteins to the carboxylate-bearing ends of the SWNTs. On the other hand, when the enzymes were placed onto SWNT forests without EDC coupling, CVs persisted for only a few repetitive scans. Additionally, when Nafion–$Fe(OH)_3$ under-layers on PG were treated with EDC and enzyme, CV peaks observed for Mb and HRP decreased to background levels within 30 min or

[37] Zhang, Zhe; Chouchane, Salem; Magliozzo, Richard S.; Rusling, James F. *Anal. Chem*. **2002**, *74*, 163.
[38] Rusling, J. F. *Electroanalytical Methods for Biological Materials,* Marcel Dekker, N.Y. **2002**, pp. 195-231.

less, suggesting only transient binding of the positively charged proteins to the Nafion–$Fe(OH)_3$ under-layer. When Mb or HRP are coupled to an electrode, a complex catalytic cycle for the reduction of H_2O_2 is set up that can be detected via catalytic reduction current[37,39].

Fig. 2-3 shows a large catalytic reduction peak when H_2O_2 was added to buffers containing the SWNT/enzyme electrodes. Addition of 0.1 mM H_2O_2 increased the peak current 5-fold, and the oxidation peak disappeared. The postulated reaction mechanism, (Fig. 2-4.)[37,39], features multiple catalytic cycles and 3 possible electrochemical reductions. H_2O_2 converts the Fe^{III} enzyme to a ferryloxy active oxidant form. This may be reduced directly at the electrode, but also reacts with H_2O_2 to give oxygen and regenerate Fe^{III} enzyme. Oxygen can react with the Fe^{II} enzyme formed at the electrode to give the Fe^{II}-O_2 enzyme, which can also be reduced. From this complex catalytic system, large amperometric signals are generated from HRP and/or Mb bound to electrodes poised at -0.3 V vs. SCE. There was a linear increase in catalytic reduction peak with increasing H_2O_2 concentration from 1 to 30 mM. Hydrodynamic amperometry provided better sensitivity of the SWNT/enzyme films for H_2O_2 (Fig. 2-5(A)).

The sensitivity to the change in the concentration of H_2O_2 as the slope of the calibration curve below 10 mM was 0:050 mA/mM for SWNT/HRP, 50% better than

[39] Munge, Bernard; Estavillo, Carmelita; Schenkman, John B.; Rusling, James F. *Chem. Bio. Chem*. **2003**, *4*, 82.

the sensitivity of SWNT/Mb at 0:040 mA/mM (Fig. 2-5(B)). This is consistent with the better peroxidase activity of HRP compared to Mb. The estimated detection limits towards H_2O_2 as three times the noise levels were ~70 nM for SWNT/Mb and ~50 nM for SWNT/HRP.

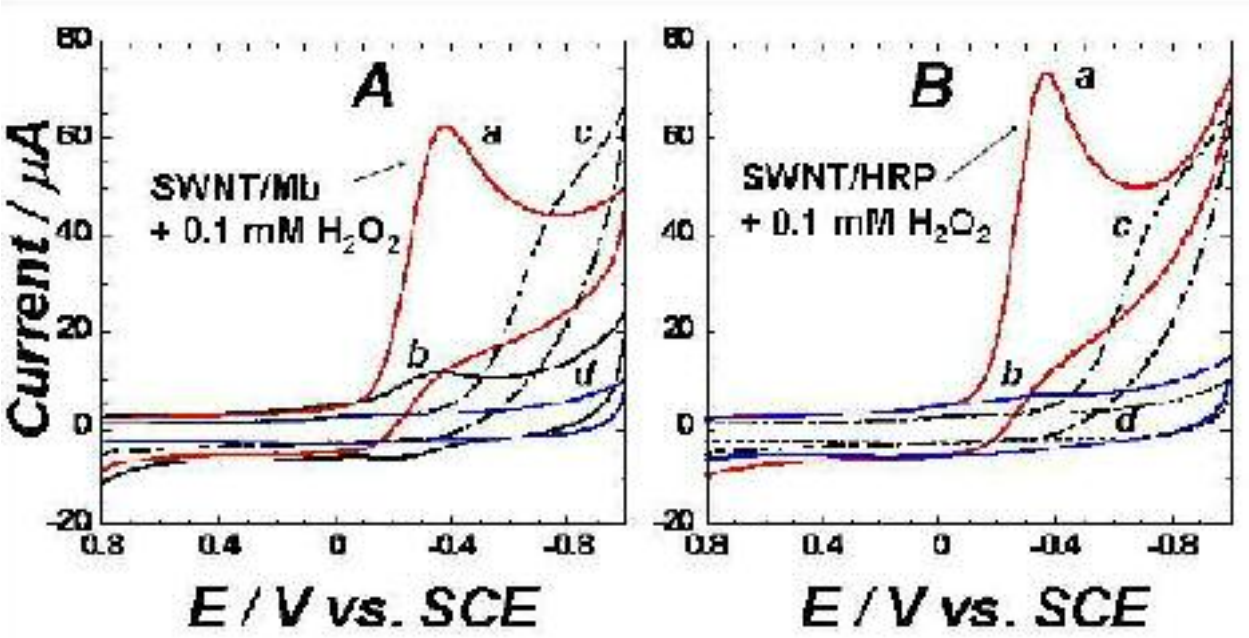

Figure 2-3. Cyclic voltammograms at 0.3 Vs^{-1} for *(A)* SWNT/Mb and *(B)* SWNT/HRP after injecting 0.1 mM H_2O_2 *(a),* SWNT/protein in anaerobic buffer pH 7.0 *(b),* SWNT control + 0.1 mM H_2O_2 *(c)* and SWNT control in anaerobic buffer pH 7.0 *(d)*.

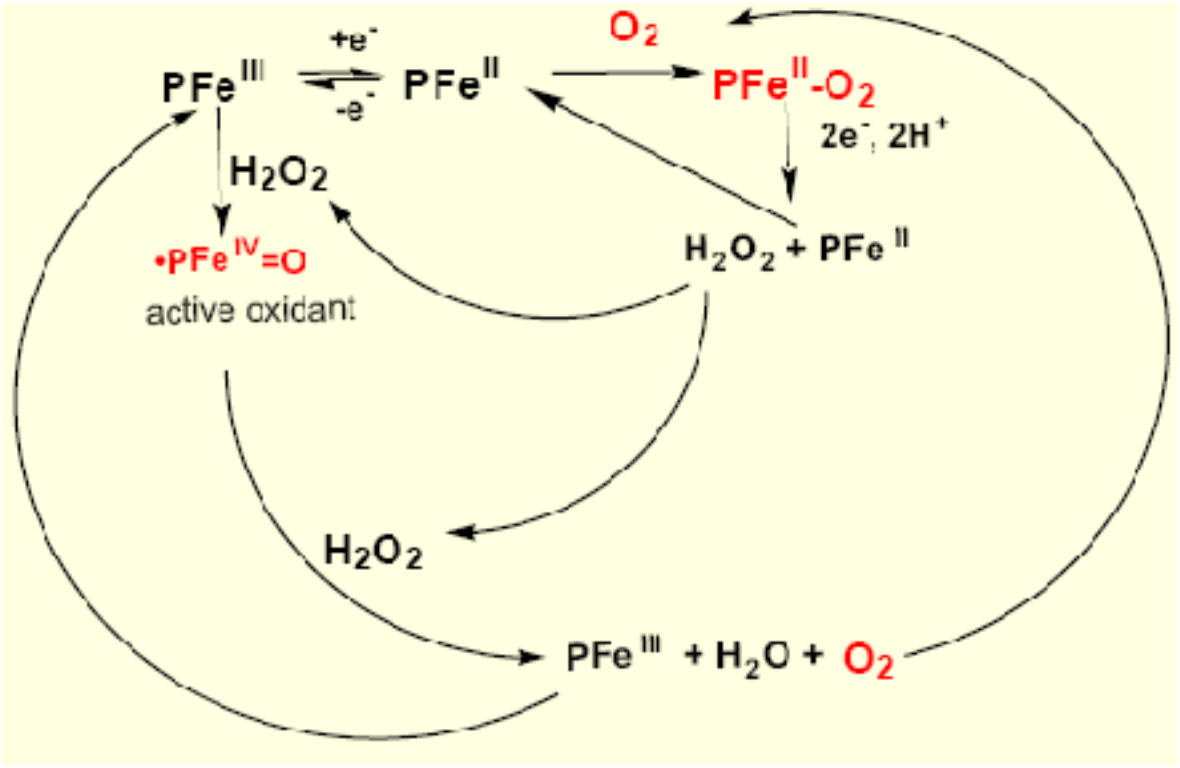

Figure 2-4. Catalytic mechanism for the peroxide (H_2O_2) reduction using HRP and/or Mb on electrodes resulting in a large amperometric signal.

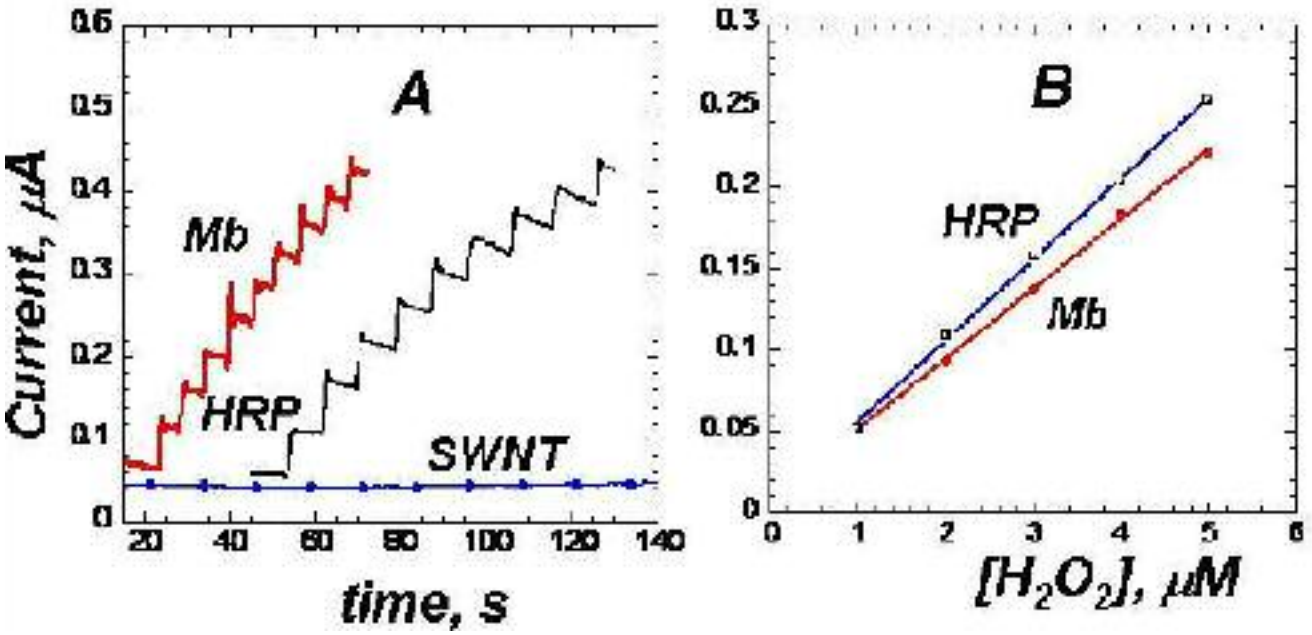

Figure 2-5. Catalytic rotating disk amperometry response at –0.3 V vs. SCE and 3000 rpm showing stepwise increase in current after injection of 1 mM H_2O_2 (A) of HRP/SWNT and Mb/SWNT, and (B) corresponding calibration curves. Slope relates to sensitivity. HRP therefore is more sensitive to redox.

2.5. Conclusions

In summary, we demonstrated the optimal conditions for fabrication of vertically aligned SWNT arrays and their application in a biosensor configuration with enzyme linked to the ends of the nanotubes. The nanotube forest behaves electrically similar to a metal, conducting electrons from the external circuit to the enzymes. The preparation of these prototype SWNT-forest biosensors is easy, and enzyme layers are stable for weeks. The oriented SWNT forests coupled to antibody-antigen biorecognition events have great potential of being fabricated as ultramicroelectrodes on the nanometer scale, for ultra-sensitive immunosensor array applications.

Chapter 3

Immunosensing of PSA using vertically aligned single-walled carbon nanotube forests

3.1 Abstract

3.2. Introduction

Prostate specific antigen (PSA), a cancer biomarker protein, is produced by normal prostate cells. It is essential to fertility and dissolution of seminal fluid[40]. Clinical research has found the protein as an important serum marker for prostate carcinoma. While no specific level designates a diagnosis of prostate cancer, PSA serum level changes over time are the most valuable way of determining if more diagnostic tests are needed[40].

[40] Brosman, Stanley A. "Prostate Specific Antigen." EMedicine From WebMD. 15 June 2006. University of California Los Angeles Medical School. 23 Mar. 2007

Currently a PSA test with a 4.0ng/mL sensitivity levels predicts cancer 67.5-80% of the time. Improving sensitivity levels to be able to detect an increase of 0.75ng/mL over a year to indicate need of biopsy would possibly prevent cancers that are missed 20-30% of the time[40]. The most current method of detection comparable to our method is the use of optimized ELISA (Enzyme-Linked Immunosorbent Assay)[41]. This method requires somewhere between 50-150μL of serum which proves to be challenging when sampling of tissue is necessary.

Our research team following a literature method[42] has self-assembled 20-30nm long terminally carboxylated single-wall carbon nanotubes (SWNT) into forests standing upright on bundles of nafion-iron oxide decorated conductive surfaces. The SWNT forests were previously fully characterized using polarized Raman spectroscopy and atomic force microscopy which confirmed the vertical orientation of the nanotubes in bundles of 20-100nm diameter at cover of >98% of the underlying solid substrate[43]. Efficient, direct electrical communication was achieved between the highly conductive nanotubes in these forests and peroxidase enzymes bioconjugated to their ends[43,44].

In our protocol, primary antibody on the SWNT sensor binds antigen in the sample, which in turn, binds a peroxidase-labeled antibody (Figure 3-1). Amperometric signals are developed by adding small amounts of hydrogen peroxide to a solution bathing the

[41] Ward, A.M.; Catto, J.W.F.; Hamdy, F.C. *Ann. Clin. Biochem.* **2001**, *38*, 633-651.
[42] Xhattopadyhyay, D. et al. *J. Am. Chem. Soc.* **2001**, *123*,9451-9452.
[43] Yu, Xin.; Kim, Sang Nyon; Papadimitrakopoulous, F.; Rusling, J. F.. *Mol. Biosys*. **2005**, *1*, 70-78.
[44] Yu, Xin; Chattopadhyay, D.; Galeska, I; Papadimitrakopoulous; F.; Rusling, J.F. *Electrochem. Comm.* **2003**, *5*, 408-411.

sensor to active the peroxidase electrochemical cycle and measuring the current for catalytic peroxide reduction while the sensor is under constant voltage[44, 45]

In this chapter, we report a novel SWNT immunosensors and applications to the detection of a cancer biomarker in clinically relevant serum samples. While label-free strategies are attractive in that they eliminate the need for antibody labeling, herein we pursue a enzyme label strategy that provides advantages of enhanced sensitivity and selectivity, the latter by virtue of requiring two specific binding events for detection.6 Decent sensitivity was achieved by this non-amplified immunosensor utilizing a bioconjugate with 1 or 2 horseradish peroxidase (HRP) labels. This resulted in a detection limit of 4 ng mL^{-1} for prostate specific antigen (PSA) in 10 µL undiluted calf serum.

3.3. Experimental Section

The fabrication of the SWNT forests on graphite tips was discussed in Chapter 2. Primary antibody was attached with use of 30µL 400mM EDC [1-(3-(dimethylamino)-propyl)-3-ethylcarbodiimide hydrochloride] and 100mM NHSS [N-hydroxysulfosuccinimide] which was washed off after a 10 minute incubation period. The electrodes were then immediately incubated at 37°C for 3 hours (optimal) with 20µL of 330 ng/mL primary

[45] O'Connor, Maire; Kim, Sang Nyon; Killard, Anthony J.; Forster, Robert J.; Smyth, Malcolm R.; Papadimitrakopoulos, Fotios; Rusling, James F. *Analyst* **2004**, *129*, 1176-1180.

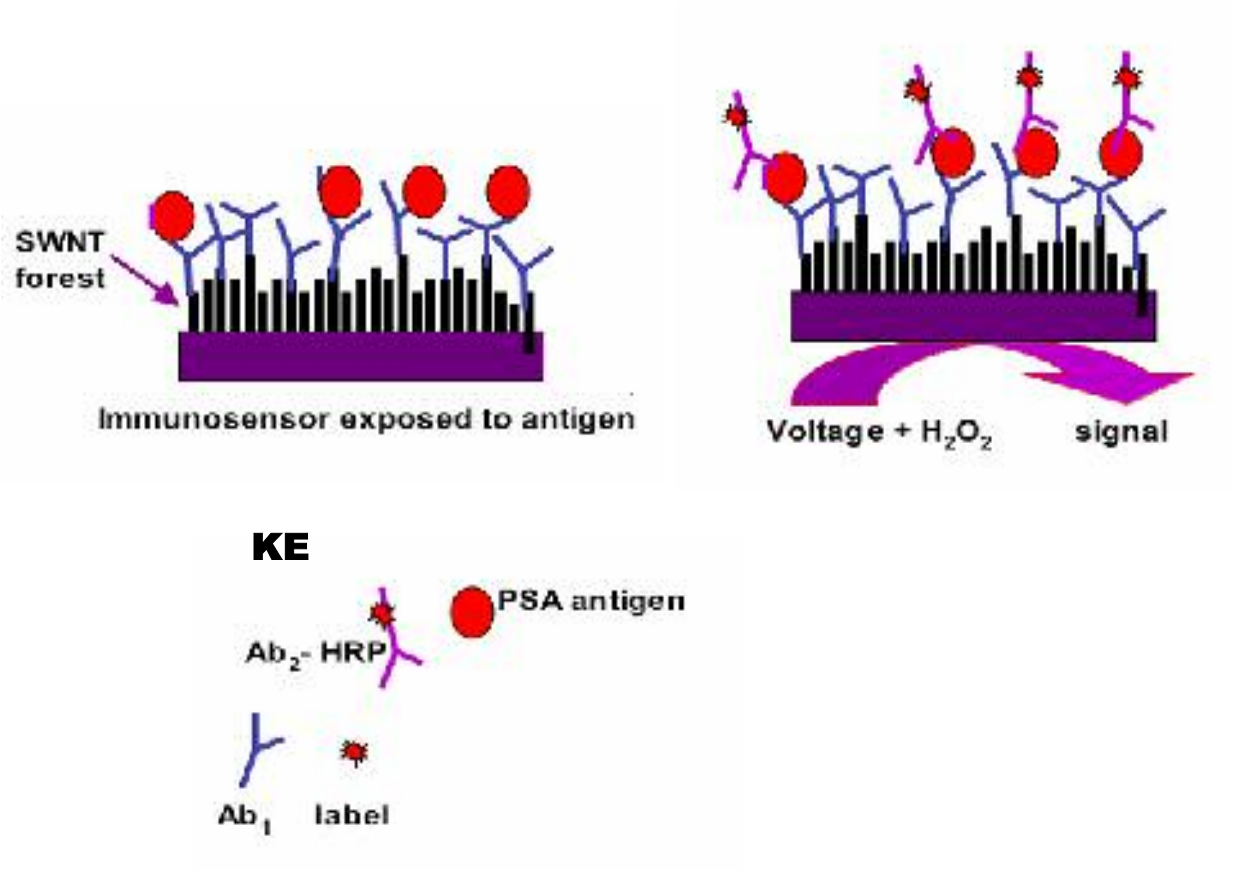

Figure 3-1. Illustration of Sandwich Immunoassay principles for SWNT Immunosensors. Initial antibody (Ab_1) is bioconjugated to the carboxylated ends of the carbon nanotube forests. (Prostate Specific Antigen) PSA is then attached to initial antibody. Finally, the HRP labeled secondary antibody (Ab_2) is attached to PSA allowing for its electrochemical detection.

anti-PSA antibody (Ab_1) in a solution of PBS buffer containing 0.05% Tween-20 at a pH of 7. After the incubation period the electrode was washed with the PBS buffer containing 0.05% Tween-20. This electrode was then incubated immediately with 20µL of 2% BSA + 0.05% Tween-20 again followed by washing with PBS buffer and 0.05% Tween-20.

The SWNT-Ab_1 electrode was then incubated at 37°C for 1hr and 15minutes with 10µL of PSA-antigen at varying concentrations. This step was again followed by washing with PBS buffer containing 0.05% Tween-20. The SWNT-Ab_1-PSA electrode was then incubated for 1 hr. 15min. at 37°C with 10µL of 4pmol/mL HRP-labeled anti-PSA antibody (Ab_2-HRP). Again the electrode was washed after incubation with PBS buffer containing 0.05% Tween-20. All washing steps were vital as they prevent non-specific binding (NSB), which would result in a false-positive amperometric detection of PSA antigen.

This working electrode containing the sandwich immunoassay was then placed in a 3-electrode cell for cyclic voltammetry and amperometry at room temperature. The cell contained 10mL of PBS buffer at pH 7 and 1mM of hydroquinone. Electrochemical signals were generated with the use of the CHI 660C electrochemical workstation. Cyclic voltammetry scans were run on each electrode to prep it for electron exchange in the amperometric detection. This provided information on the redox ability of the electrode prior to amperommetry. Amperometric detection was then run at -0.3V with the working

electrode rotated at 3000rpm. Micromolar injections of 0.4mM H_2O_2 were used to generate the stepwise signal.

3.4. Results and Discussion

Prostate specific antigen (PSA) is a biomarker for prostate carcinoma, and is an established clinical tool for diagnosing and monitoring the disease.[30] We first analyzed undiluted calf serum containing different amounts of PSA with the SWNT immunosensors with anti-PSA attached (Figure 3-2). Inhibition of nonspecific binding (NSB) was critical to achieve the best sensitivity and detection limits. Thus, we developed a highly effective blocking procedure utilizing competitive binding of bovine serum albumin (BSA) and the detergent Tween-20, and also optimized the concentration of tracer secondary anti-PSA antibody (Ab_2-HRP) (see Experimental Section). Before exposure to the sample, immunosensors were incubated for 1 h with 20 mL 2% BSA + 0.05% Tween-20, then washed with 0.05% Tween-20 in buffer. For measurements, 10 mL undiluted new born calf serum containing PSA was incubated on the inverted sensor surface, blocking buffer was used to wash; then the sensor was incubated with 10 mL HRP-labeled secondary anti-PSA. The washed immunosensor was then placed into an electrochemical cell containing the mediator hydroquinone in buffer, and hydrogen peroxide was injected for signal development (Figure 3-2).

The steady state current increased linearly (Figure 3-3) with PSA concentration over the range 0.4-40 ng mL-1, encompassing the 4-10 ng mL-1 prostate cancer prediction range for human serum. Excellent device-to-device reproducibility is illustrated by the small error bars, and sensitivity of 9.88 nAmL ng $^{-1}$ (Figure 3-3B) was achieved. The detection

limit of 0.4 ng mL^{-1} as the zero PSA control signal plus three-times the control noise level (Figure 3-2 inset) was similar to that obtained for PSA in buffers (not shown). Results indicate that using BSA and detergent for NSB blocking, and optimizing the concentration of Ab_2-HRP is very effective to minimize NSB in serum. Control experiment, Figure 3-2 inset, represents a SWNT immunosensor taken through the full procedure without exposure to PSA, and the response reflects the sum of residual NSB and direct reduction of hydrogen peroxide. The controls with no PSA responses were significantly smaller than full immunoassay with the lowest PSA concentration, 0.4 $ngmL^{-1}$. Results described above with this non-amplified SWNT immunosensors show that we can accurately detect cancer biomarkers in complex biological samples with very good sensitivity and selectivity (Figures 3-2 and 3-3). Further, the immunosensors have a very good reproducibility, as demonstrated by device-to-device standard deviations.

3.5. Summary

In summary, we have demonstrated a sensitive and selective electrochemical detection of a protein cancer biomarker with SWNT immunosensors, as exemplified by the measurement of PSA in clinically relevant serum samples. The detection limit of 4 ng mL-1 for this non-amplified SWNT immunosensor compares favorably with the standard enzyme linked immunosorbent assay (ELISA). This SWNT immunosensors can be adapted easily for the detection of other relevant biomarkers and have the potential for fabrication into arrays to facilitate multiplexed detection. We believe that such devices will evolve toward a very promising future for reliable point-of-care diagnostics of cancer and other diseases, and as tools for intra-operation pathological testing, proteomics, and

.

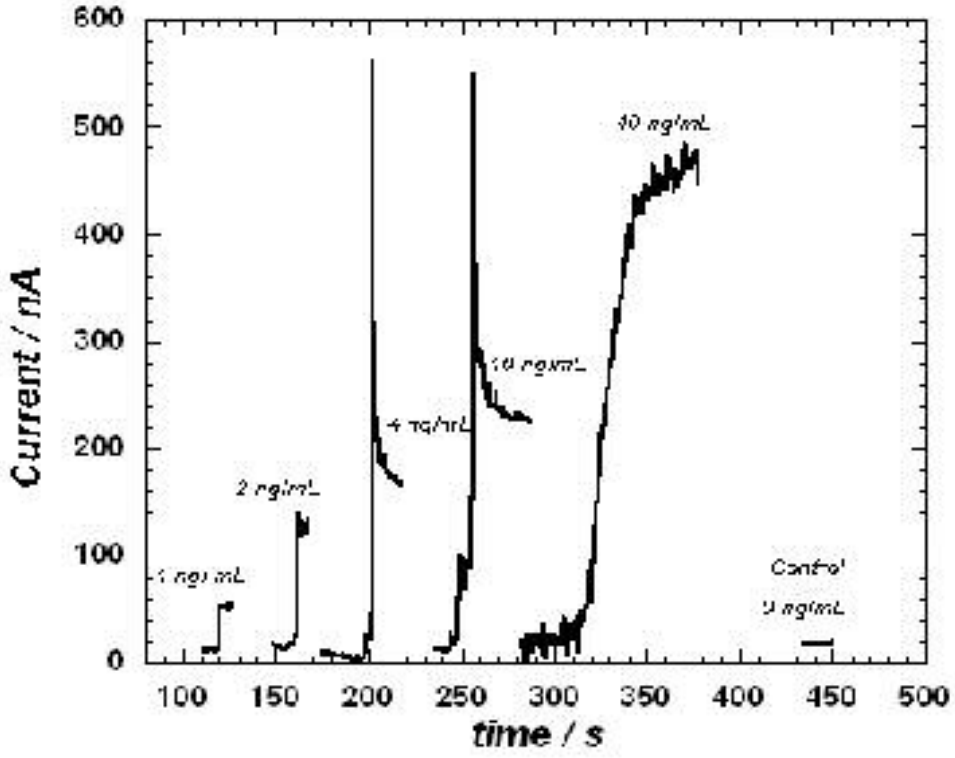

Figure 3-2A. Amperometric signal generation for SWNT immunosensors incubated with varying concentrations of PSA antigen. Current levels at -0.3V vs. SCE and 3000rpm rotation.

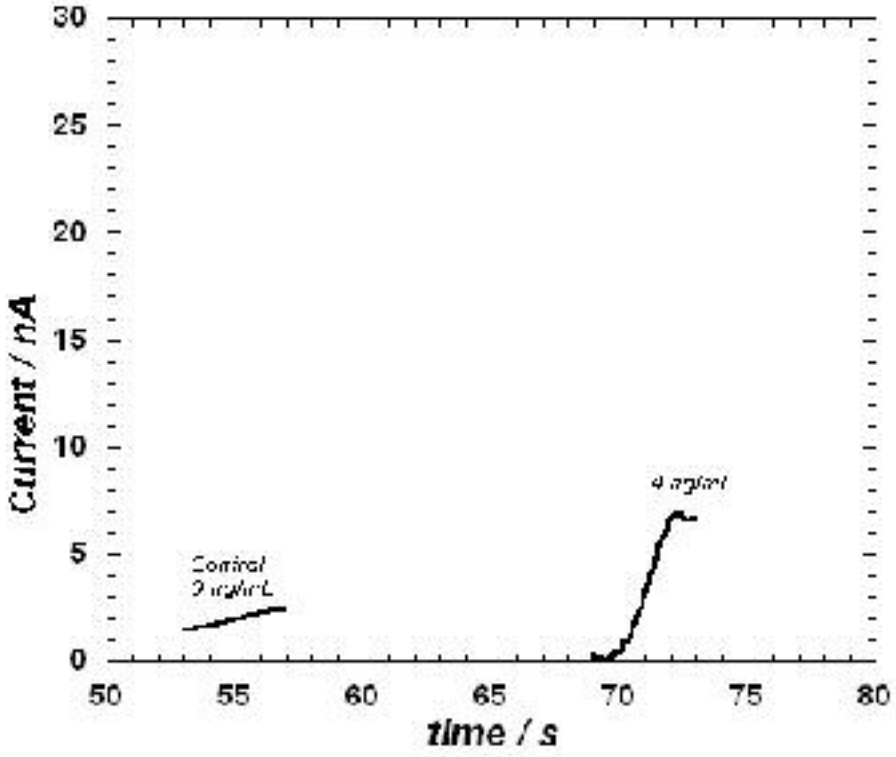

Figure 3-2B. Amperometric signal generation for SWNT immunosensors at detection limits. Current levels at -0.3V vs. SCE and 3000rpm rotation.

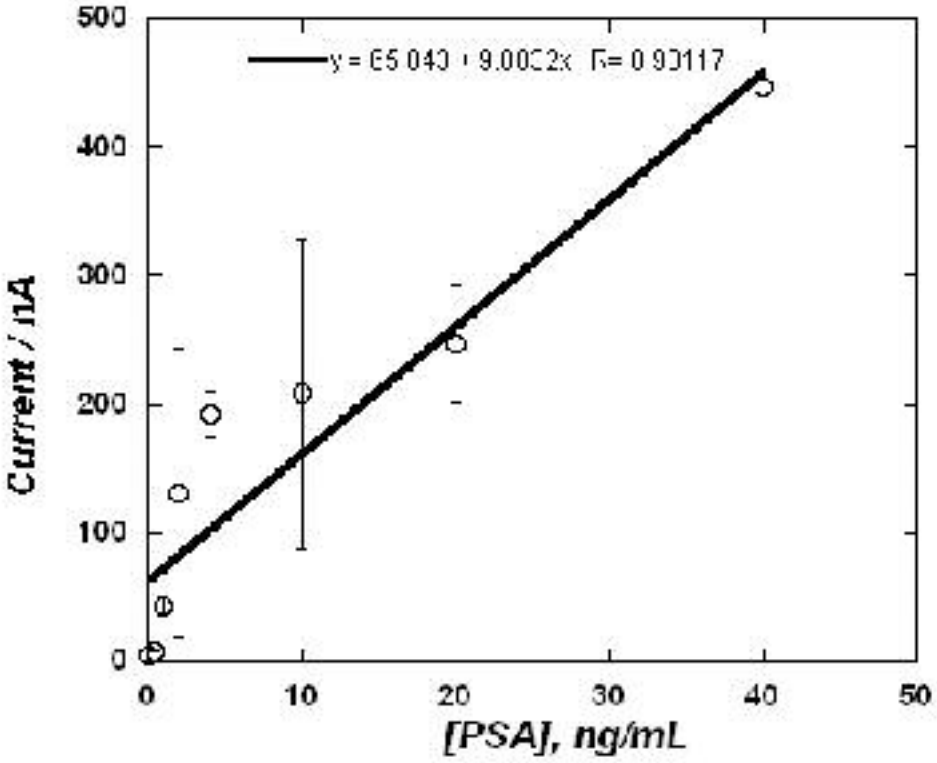

Figure 3-3. Influence of PSA concentration on amperometric signal. Error bars indicate standard deviation of values.

systems biology. Work is in progress in our lab to lower the detection limits using signal amplification strategies.

Chapter 4

The Pell Scholars Honors Program Connection

4.1 Connection

The Pell Honors program was created in conjunction with retired United States Senator Claiborne DeBorda Pell and Salve Regina University. During Mr. Pell's Senate career he spent 34 years on the Foreign Relations Committee; always true to the founding principles of the United Nations in his work. In honor of his life and work the Pell Program was formed to create a network of students from different disciplines that would focus a portion of their studies on international relations and public policy, placing an emphasis on a sense of civic responsibility[46]. In light of this, my senior thesis focused on the electrochemical detection of protein biomarkers, expressly prostate specific antigen, for use in the identification of prostate cancer. This technology has the potential for a wide range of applications. Hopefully, with these detection protocols the future costs of disease treatment will be lowered as diagnoses of disease will occur much earlier.

With the exception of skin cancer, prostate cancer is the most commonly diagnosed cancer in American men and second leading cause of cancer deaths. 20% of men will develop prostate cancer that is invasive before death. Currently digital rectal exams

[46] "The Pell Scholars Honors Program." The Pell Center for International Relations and Public Policy. 2007. Salve Regina University. 10 Mar. 2007<http://www.salve.edu/pellcenter/scholars.cfm#overview>.

(DREs) in conjunction with tests for the protein serum marker Prostate Specific Antigen (PSA) are the methods employed in diagnoses of this disease[47].

The cost of treatment for such a devastating disease can be very high. The cost by definition encompasses physician and healthcare professionals, care provided by hospitals, drugs, and laboratory services[48]. Many studies have been conducted to determine the cost-benefit of early cancer detection. Figure 4-1 and Figure 4-2 describe the benefit-cost equation and its variables as determined by the *Cancer Journal for Clinicians*.

The data provided by the *Cancer Journal for Clinicians* indicates at current a negative benefit-cost of screening for individuals as the current cost of testing outweighs the benefits mathematically. The current data of this study indicates that early detection could be more economical through a more specific PSA assay[49]. A population that is growing older also indicates a higher incidence of disease in the future[50].

[47] Ferrini, Rebecca, and Steven Woolf. "Screening for Prostate Cancer in American Men." American College of Preventive Medicine. 10 Mar. 2007 <http://www.acpm.org/prostate.htm>.
[48] Grover, Steven, Hanna Zowall, Louis Coupal, and Murray Krahn. *CMAJ: Canadian Medical Association Journal,* **1999,** *160.*
[49] Littrup, P.J.; Goodman, A.C.; Mettlin, C.J.; *CA: Cancer J Clin*, **1993**, *43*, 134-149.
[50] Norlund, A.; Alvegard, T.; Lithman, T.; Merlo, J.; Noreen, D.; *Scand J Urol Nephrol*, **2003**, *37*, 371-375.

$$V=pnwB + (1-p)cR - S - [pn+ (1-p)(1-c)]w(T+A) - (1-p)(1-c)F$$

Dollar Values

V	Net benefit per individual screened
B	Value of benefits from early detection and treatment
R	Value of reassurance from a negative test
S	Cost of screening test, procedure, or scenario
T	Costs of staging and treatment received as a result of screening
A	Cost of adverse effects of screening tests and subsequent follow-up tests and morbidities of therapy
F	Potential psychic cost of false-positive results

Probabilities

p	Prevalence of prostate cancer (fraction of patients who demonstrate cancer during screening sequence, as well as from interval detection)
n	Sensitivity (probability of a positive results when clinically detectable cancer is present)
c	Specificity (probability of a negative result when no cancer is evident from the screening test or sequence)
w	Probability of a patient returning for therapy and/or having a cancer stage or medical condition appropriate for therapy

Figure 4-1. Benefit-cost equation of prostate cancer screening with definition of variables[49].

Parameter Values for Benefit-Cost Analysis											
	B	**R**	**A**	**T**	**A**	**F**	**p**	**n**	**c**	**q**	**V**
DRE (highly skilled examiner)	$29,443	$90	$90	$20,000	$1,391	$1,391	0.053	0.606	0.963	0.85	-$474
DRE (generalized)	$29,443	$90	$90	$20,000	$1,391	$1,391	0.053	0.484	0.77	0.85	-$4,112
DRE + PSA 2ng/mL	$29,443	$180	$180	$20,000	$1,470	$1,470	0.053	0.96	0.688	0.85	-$5,544
DRE + PSA 3ng/mL	$29,443	$180	$180	$20,000	$1,438	$1,438	0.053	0.899	0.827	0.85	-$2,936
DRE + PSA 4ng/mL	$29,443	$180	$180	$20,000	$1,421	$1,421	0.053	0.869	0.896	0.85	-$1,645
PSA 2ng/mL	$29,443	$90	$90	$20,000	$1,477	$1,477	0.053	0.909	0.705	0.85	-$5,126
PSA 3ng/mL	$29,443	$90	$90	$20,000	$1,436	$1,436	0.053	778	0.853	0.85	-$2,473
PSA 4ng/mL	$29,443	$90	$90	$20,000	$1,413	$1,413	0.053	0.667	0.927	0.85	-$1,126
Mammography	$29,443	$50	$50	$20,000	$1,450	$1,450	0.005	0.8	0.97	0.99	-$562

Figure 4-2. Benefit-cost equation of prostate cancer screening variable values[49].

This indicates a need for a better method of PSA detection that would be available at a lower cost which would make screening accessible to a larger portion of the population. Our current research is looking to create an effective sensitive and cost effective method for PSA analysis leading to earlier and more accurate detection. In the future, not only will PSA be detected for but also multiple biomarkers proteins including PF_4 and MMP2 that are currently under investigations in our lab. As a result of this technology, hopefully a dramatic decrease in prostate cancer deaths will occur.

Acknowledgements

First and foremost I would like to thank **Dr. Bernard Munge** for the opportunity to be a part of this remarkable project. The lessons I have learned not only about my topic but about the research process itself will prove to be invaluable in my future endeavors.

Thank you to **Dr. Stephen Trainor** and **Dr. Paula Martasian** for your advice and supervision throughout my experience with Pell Program.

Also thank you to **Dr. Sandor Kadar** for four years of continual guidance.

This project would not have been possible without the incredible help of my colleagues **Jaqueline Fisher, Phelipe Hurt, Andrew Hall, Colleen Krause,** and **Lines Millord**.

Finally, I wish to acknowledge the financial support from the National Center for Research Resource, a component of the *National Institute of Health (NCRR/NIH)*

LIST OF FIGURES

Figure 1-1. Prostate Specific Antigen structure as determined by x-ray diffraction……..….12

Figure 1-2. Two types of carbon nanotubes; SWNT & MWNT…….…….13

Figure 1-3. Heme group of Horseradish Peroxidase...……...15

Figure 2-1. Schematics of the fabrication protocol of the vertically aligned SWNT arrays. End carboxyl group on the SWNT allow protein bioconjugation facilitating electron shuttle to active protein redox sites.……20

Figure 2-2. Raman spectra (A) showing characteristic D bands, G band and RBM band of SWNT assembled on PG electrodes and the influence of $Fe(Cl)_3$ solution pH during SWNT assembly, and (B) AFM image of the resulting vertically aligned SWNT arrays on Si wafers at the optimal pH 1.7.……22

Figure 2-3. Cyclic voltammograms at 0.3 Vs-1 for *(A)* SWNT/Mb…….25
and *(B)* SWNT/HRP after injecting 0.1 mM H_2O_2 *(a),*
SWNT/protein in anaerobic buffer pH 7.0 *(b),* SWNT
control + 0.1 mM H_2O_2 *(c)* and SWNT control in anaerobic
buffer pH 7.0 *(d)*

Figure 2-4. Catalytic mechanism for the peroxide (H_2O_2) reduction…….. 26
using HRP and/or Mb on electrodes resulting in a
large amperometric signal.

Figure 2-5. Catalytic rotating disk amperometry response at……..…….27
–0.3 V vs. SCE and 3000 rpm showing stepwise
increase in current after injection of 1 mM H2O2
(A) of HRP/SWNT and Mb/SWNT, and (B)
corresponding calibration curves**.**

Figure 3-1. Illustration of Sandwich Immunoassay principles…….……33
for SWNT Immunosensors.

Figure 3-2A. Amperometric signal generation for SWNT…….…….37
immunosensors incubated with varying concentrations
of PSA antigen. Current levels at -0.3V and
3000rpm rotation.

Figure 3-2B. Amperometric signal generation for SWNT immunosensors……..……..38
at detection limits. Current levels at -0.3V vs. SCE and
3000rpm rotation.

Figure 3-3. Influence of PSA concentration on amperometric signal……..……39
Error bars indicate standard deviation of values.

Figure 4-1. Benefit-cost equation of prostate cancer screening with……..…….44
definition of variables.

Figure 4-2. Benefit-cost equation of prostate cancer screening……...……45
variable values.